Computer Optimal Control of Batch Polymerization Reactor

3 AUTHORS:

Sathy Ponnuswamy
SunEdison
14 PUBLICATIONS **205** CITATIONS

SEE PROFILE

Sirish Shah
University of Alberta
336 PUBLICATIONS **5,824** CITATIONS

SEE PROFILE

Costas Kiparissides
Aristotle University of Thessaloniki
324 PUBLICATIONS **4,903** CITATIONS

SEE PROFILE

Computer Optimal Control of Batch Polymerization Reactors[†]

Saty R. Ponnuswamy and Sirish L. Shah

Department of Chemical Engineering, University of Alberta, Edmonton, Canada T6G 2G6

Costas A. Kiparissides*

Department of Chemical Engineering, University of Thessaloniki, Thessaloniki, Greece

This paper presents a theoretical and experimental analysis of the open- and closed-loop optimal control of a batch reactor for the solution polymerization of methyl methacrylate. A novel experimental reactor system with facilities for on-line measurements of polymer quality is employed to verify the theoretical results. A process control computer is used for on-line data acquisition and implementation of the time optimal policies. These policies are derived by application of the Maximum Principle to a mathematical model of the process. Experimental results show good agreement with theoretical predictions. Optimal closed-loop control policies are also derived and implemented on a simulated reactor model. It is shown that the multivariable feedback controller is able to track the nominal open-loop optimal state trajectories in the presence of process disturbances.

Significant economic advantages can be obtained by operating polymerization reactors in an optimal way such that consistent product quality is maintained or/and the polymerization time is minimized. The state of the art and the benefits of automation and computer control of polymerization reactors have been discussed in detail in three excellent review papers by Amrehn (1977), Hoogendoorn and Shaw (1980), and MacGregor et al. (1983).

Although computer automation has been successfully applied to the polymerization industry over the past 15 years, the progress in computer optimal control of polymerization reactors has been slow. This has been mainly attributed to the lack of robust and reliable on-line polymer characterization devices. In the past, closed-loop control in polymerization reactors was limited to temperature and pressure control. However, with the advent of advanced computer control techniques and the development of new analytical techniques for measurement of polymer quality, the scope of on-line control of polymer quality has largely increased.

Most of the previous studies on open-loop optimal control of polymerization reactors dealt with theoretical predictions of time optimal temperature and initiator addition policies required to produce a polymer with desired molecular weight averages in minimum time (Yoshimoto et al., 1971; Hicks et al., 1969; Sacks et al., 1972, 1973; Chen and Jeng, 1978; Chen and Lin, 1980; Chen and Huang, 1981; Farber, 1983; Tsoukas et al., 1982; Thomas and Kiparissides, 1984). In spite of all these theoretical developments, there are only a few published reports on the actual implementation of such optimal policies to experimental reactor systems (Chen and Huang, 1981; Chen and Hsu, 1984; Wu et al., 1980; Tirrell and Gromley, 1981).

Compared to the open-loop optimal control studies, optimization of polymer quality through feedback control has been largely limited by the lack of on-line polymer characterization instruments. In fact, as pointed out by Hoogendoorn and Shaw (1980), the measuring instruments are often the weakest link in any polymerization closed-loop control study.

From the above, it is apparent that more research is needed in the areas of on-line measurements and computer optimal control of polymerization reactors. The present paper deals with the theoretical and experimental application of optimal control theory to the free-radical solution polymerization of methyl methacrylate in a batch reactor. The experimental facility, which includes a number of on-line measurement devices and a real-time computer, is described in the following section. Subsequently, different open-loop optimal policies are derived for the batch reactor. These optimal policies are implemented on the experimental reactor system, and the results are compared with the theoretical predictions. Finally, the closed-loop control problem is solved to calculate the optimal feedback control law which can maintain the process variables along the established open-loop optimal state trajectories in the presence of process disturbances.

Reactor and Computer System

A schematic representation of the experimental system is shown in Figure 1. The jacketed glass reactor has a capacity of 5 L and is provided with a stirrer for thorough mixing of the reactants. Heating of the reaction mixture is achieved by circulating hot water through the reactor jacket. Cooling, as required during the exothermic stage of the reaction, is carried out by cold water flowing through a stainless steel coil placed inside the reactor. A PI controller is used to maintain the desired temperature inside the reactor by manipulating the flow rate of the cooling water. The controller has a provision to accept remote set-point values, a facility that is used in the optimal computer control studies.

During polymerization, the reaction mixture is continuously circulated through an on-line densitometer for measurement of monomer conversion (Schork and Ray, 1981; Ponnuswamy et al., 1986a). From the densitometer, the reaction mixture flows through a three-way solenoid valve back to the reactor. An automatic sampling system that periodically collects a polymer sample and prepares it for molecular weight analysis has been developed. The essential features of the sampling system and its microprocessor-based operation are described by Ponnuswamy (1984). A size exclusion chromatograph (SEC) monitors the molecular weight distribution (MWD) during polymerization (Ponnuswamy et al., 1986b).

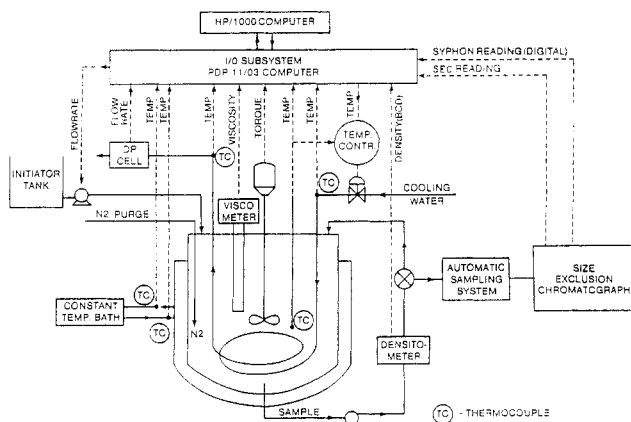Even though MWD can be measured by the on-line SEC

Figure 1. Schematic diagram of polymerization reactor system.

detector, this measurement involves a time delay of about 10–15 min. Thus, an on-line falling piston industrial viscometer mounted on the reactor lid is also employed to obtain an almost continuous measurement of the viscosity of the reaction mixture. The molecular weight of the polymer can be then calculated from an empirical correlation involving viscosity, polymer concentration, molecular weight, and temperature.

The torque exerted on the constant rpm stirrer is also measured to obtain an indirect measurement of molecular weight changes in the reactor. Finally, a Hewlett-Packard (HP/1000) minicomputer is employed for data acquisition and control of the experimental reactor. A detailed evaluation of the performance of the various on-line measuring devices has been reported by Ponnuwamy et al. (1986a).

The free-radical solution polymerization of methyl methacrylate (MMA) was selected to study the problems related with computer control of polymerization reactors. Commercial monomer MMA was vacuum-distilled to remove the inhibitor. Toluene was chosen as a solvent because of its high boiling point. The initiator, benzoyl peroxide, was dissolved in chloroform and recrystallized in methanol before use. The reactor was purged with nitrogen during polymerization to prevent oxygen from being dissolved into the reaction mixture. A number of experiments were conducted to study the effects of solvent volume fraction (Φ_s: 0.4–06), temperature (60–75 °C), and initial initiator concentration (0.05–0.10 g-mol/L) on the monomer conversion and MWD. The experimental measurements were then used to estimate the kinetic parameters of the free-radical solution polymerization of MMA (Ponnuswamy, 1984).

A variety of optimization problems can be formulated for a batch free-radical polymerization reactor. The problems differ in the definition of the objective function and the selection of the control variables. In free-radical polymerization, the reaction temperature and the concentrations of initiator and chain-transfer agent are usually chosen as controlled variables. These variables can affect the rate of polymerization and the molecular weight of the polymer.

In this work, three different optimization problems have been formulated and solved for a batch reactor for the solution polymerization of methyl methacrylate. The theoretical calculation of the various time optimal policies and their experimental verification are discussed in the following sections.

The Minimum-Time Optimal Initiator Policy

The objective of this problem is to calculate an optimal initiator policy for a given reaction temperature that

minimizes the reaction time, t_f, required to achieve a desired final monomer conversion, X_d, and a desired number-average molecular weight, $\bar{M}_{nd}$. Needless to say, the final desired values of X_d and $\bar{M}_{nd}$ must belong to the set of reachable states by the control variable.

Assuming constant density and applying the quasi-steady-state approximation for live radicals, the following mass balance equations can be written for a batch MMA free-radical solution polymerization reactor (Ray, 1967; Ponnuswamy, 1984):

$$dI/dt = -k_d I \qquad (1)$$

$$dM/dt = -k_1 M I^{1/2} \qquad (2)$$

$$d\mu_0/dt = k_4 k_d I + k_2 M I^{1/2} + k_3 S I^{1/2} \qquad (3)$$

$$d\mu_2/dt = (k_s S + k_m M)\lambda_2 + k_t \lambda_0 \lambda_2 + k_{tc} \lambda_1^2 \qquad (4)$$

where

$$\lambda_0 = (2 f k_d I / k_t)^{1/2} \qquad (5)$$

$$\lambda_1 = \frac{2 f k_d I + (k_p M + k_m M + k_s S)\lambda_0}{k_m M + k_s S + k_t \lambda_0} \qquad (6)$$

$$\lambda_2 = \lambda_1 + (2 k_p M \lambda_1)/(k_m M + k_s S + k_t \lambda_0) \qquad (7)$$

$$k_1 = k_p (2 f k_d / k_t)^{1/2} = A_1 \exp(-E_1/RT) \qquad (8)$$

$$k_2 = k_m (2 f k_d / k_t)^{1/2} = A_2 \exp(-E_2/RT) \qquad (9)$$

$$k_3 = k_s (2 f k_d / k_t)^{1/2} = A_3 \exp(-E_3/RT) \qquad (10)$$

$$k_4 = 2 f(1 - \nu/2) \qquad \nu = k_{tc}/k_t \qquad (11)$$

All symbols are defined in the Nomenclature section. The monomer conversion and the number- and weight-average molecular weights are given by

$$X = (M_0 - M)/M_0 \qquad (12)$$

$$\bar{M}_n = (MW)M_0 X/\mu_0 \qquad \bar{M}_w = (MW)\mu_2/(M_0 X) \qquad (13)$$

Accordingly, the minimum-time optimal initiator control problem can be formulated as follows. Given the initial and final values of the state variables M and μ_0,

$$M(0) = M_0 \qquad \mu_0(0) = 0 \qquad (14)$$

$$M_d(t_f) = M_0(1 - X_d)$$
$$\mu_{0d}(t_f) = (MW)M_0 X_d/\bar{M}_{nd} \qquad (15)$$

determine an admissible initiator control policy, I^*, which causes the nonlinear system eq 2 and 3 to follow some admissible trajectories, M^* and μ_0^*, that minimize the performance index, J,

$$J = \int_0^{t_f} dt \qquad (16)$$

For a free final time, t_f, the classical calculus of variations leads to the following solution. Define the Hamiltonian in terms of eq 2, 3, and 16 (Sage, 1968):

$$\mathcal{H} = -1 - p_1 k_1 M I^{1/2} + p_2[k_4 k_d I + k_2 M I^{1/2} + k_3 S I^{1/2}] \qquad (17)$$

where p_1 and p_2 are the costate variables, which satisfy the canonical equations

$$dp_1/dt = -\partial \mathcal{H}/\partial M = p_1 k_1 I^{1/2} - p_2 k_2 I^{1/2} \qquad (18)$$

$$dp_2/dt = -\partial \mathcal{H}/\partial \mu_0 = 0 \qquad (19)$$

Note that p_2 will be a constant. If the control variable, I, is unconstrained, the optimal policy for I, which maximizes the Hamiltonian, must satisfy the following necessary conditions (Sage, 1968):

$$\mathcal{H} = 0 \qquad \partial \mathcal{H}/\partial I = 0 \qquad \partial^2 \mathcal{H}/\partial I^2 < 0 \qquad (20)$$

Table I. Optimal Initiator Policies: Comparison of Theoretical and Experimental Results

run	temp, °C	X_d (X_f)	$\bar{M}_{nd}$ ($\bar{M}_{nf}$)	I^* (I), mol/L	t_f, min
1	65	0.50 (0.46)	5×10^5 (4.8×10^5)	0.104 (0.100)	161 (161)
2	70	0.50	5×10^5	0.0735	109
3	75	0.50 (0.49)	5×10^5 (4.8×10^5)	0.052 (0.050)	74 (74)

From the definition of the Hamiltonian eq 17 and eq 20, we obtain

$$I = -1/(k_4 k_d p_2) = \text{constant} \tag{21}$$

and

$$\partial^2 \mathcal{H} / \partial I^2 = -2I^{-2} < 0 \tag{22}$$

Thus, the optimal policy (eq 21) will maximize the Hamiltonian and make it equal to zero. This means that, for a given temperature, the optimal initiator concentration will remain constant during the course of polymerization. The optimal initiator concentration is calculated next.

For a constant initiator concentration, eq 2 and 3 can be integrated analytically to give

$$\ln (M/M_0) = \ln (1 - X) = -k_1 I^{1/2} t \tag{23}$$

$$\mu_0 = k_4 k_d I t + \frac{k_2}{k_1}(M_0 - M) + \frac{k_3}{k_1} S \ln (M_0/M) \tag{24}$$

Let X_d and $\bar{M}_{nd}$ be the desired final values for conversion and number-average molecular weight, respectively. By combination of eq 8–13 and 23 and 24, we obtain the following expressions for the final time, t_f, and the optimal initiator concentration, I^*:

$$t_f = \frac{k_t(1 - \nu/2)[\ln (1 - X_d)]^2}{k_p[k_p M_0 X_d(\text{MW})/\bar{M}_{nd} + k_s S \ln (1 - X_d) - k_m M_0 X_d]} \tag{25}$$

$$I^* = \frac{[k_p M_0 X_d(\text{MW})/\bar{M}_{nd} + k_s S \ln (1 - X_d) - k_m M_0 X_d]^2}{(1 - \nu/2)^2 2f k_d k_t[\ln (1 - X_d)]^2} \tag{26}$$

Given the values of X_d and $\bar{M}_{nd}$, the optimal initiator concentration, which is constant for a given polymerization temperature, can be calculated from eq 26. The minimum time is obtained from eq 25.

Since the initiator dissociates during the course of polymerization, fresh initiator has to be continuously added to the reactor to maintain the initiator concentration at its optimal value, I^*. Assuming that the continuous addition of initiator results in a negligible volume change, then the optimal initiator feed rate will be equal to

$$F^* = V k_d I^* = \text{constant} \tag{27}$$

For a very slow initiator decomposition rate, the initiator concentration remains almost constant throughout the polymerization. In this case, the time optimal initiator policy turns out to be a single optimal charge of initiator at the beginning of polymerization.

In Table I, optimal initiator policies are given for three polymerization temperatures. These simulations show that the optimal initiator concentration and the final time decrease as the polymerization temperature increases. This suggests that the polymerization time for given values of X_d and $\bar{M}_{nd}$ can be reduced by using an optimal initiator concentration policy at the maximum possible polymerization temperature. An experimental verification of the optimal initiator policies was made for runs 1 and 3 of Table I. The numbers inside the parentheses in Table I show the experimental values of X_f and $\bar{M}_{nf}$ at the end of the minimum polymerization time, t_f. Apparently, there is good agreement between the calculated and experimental results. Note that the initiator concentrations used in the experimental runs were slightly lower than the calculated optimal values.

The Minimum-Time Optimal Temperature Policy

The objective of this problem is to calculate the time optimal temperature policy for a given initial initiator concentration to produce a polymer with desired final X_d and $\bar{M}_{nd}$ in minimum time. This problem was originally solved by Sacks et al. (1973) for the free-radical polymerization of styrene and MMA in a batch reactor. They found that the optimal temperature policy should keep the rate of production of primary radicals constant.

In this problem, the objective function can be expressed in terms of the final time and the weighted sum of squares of deviations of M and μ_0 from their corresponding desired values M_d and μ_{0d}

$$J = \int_0^{t_f} dt + w_1[M(t_f) - M_d]^2 + w_2[\mu_0(t_f) - \mu_{0d}]^2 \tag{28}$$

where w_1 and w_2 are proper weights. The Hamiltonian for this problem is defined in terms of the model eq 1–3 and eq 28 as

$$\mathcal{H} = -1 - p_1 k_d I - p_2 k_1 M I^{1/2} + p_3(k_4 k_d I + k_2 M I^{1/2} + k_3 S I^{1/2}) \tag{29}$$

where the costate variables p_1, p_2, and p_3 must satisfy the following canonical equations and transversality conditions:

$$\dot{p} = -\partial \mathcal{H}/\partial Y \tag{30}$$

$$p(t_f) = \partial G(Y(t_f), t_f)/\partial Y(t_f) \tag{31}$$

where G denotes the sum of the square terms in eq 28. Furthermore, if the control variable, T, is unconstrained, the time optimal temperature policy which maximizes the Hamiltonian must satisfy the following necessary conditions:

$$\mathcal{H} = 0 \tag{32}$$

$$\partial \mathcal{H}/\partial T = 0 \qquad \partial^2 \mathcal{H}/\partial T^2 < 0 \qquad T = T^* \tag{33}$$

Calculation of the time optimal temperature policies requires the solution of a two-point boundary value problem (TPBV) for the state and costate differential equations 1–3 and 30, with three initial values for $Y(0)$ and three final values for $p(t_f)$ given by eq 31, while maximizing the Hamiltonian, $\mathcal{H}$, eq 33. Several numerical methods are available for the solution of these types of problems (Kirk, 1970; Sage, 1968). In this work, a gradient method was utilized to calculate the minimum time optimal temperature policies. Computational details concerning the application of the particular method are given in Thomas and Kiparissides (1984) and Ponnuswamy (1984).

To avoid the iterative numerical solution of the TPBV problem, an alternative procedure was developed that significantly simplified the calculation of the optimal policies. In this development, an approximate model of the batch reactor was obtained by neglecting transfer reactions to monomer and solvent. Earlier simulation studies showed that neglecting transfer reactions did not affect conversion values, whereas molecular weight results could vary up to 10% from the results obtained by using the full reactor model, eq 1–4. In Appendix I, the time optimal temperature policies are derived by using the approximate
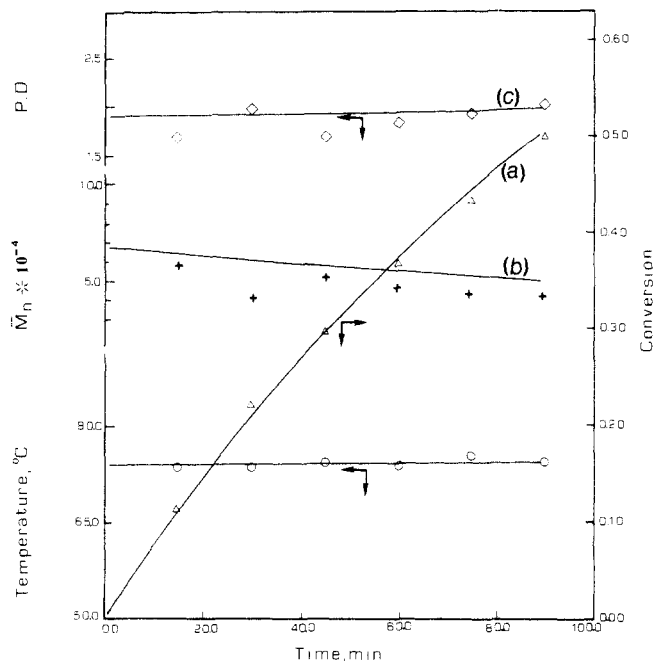
Figure 2. Comparison of theoretical and experimental results for a minimum-time optimal temperature policy (X_d = 0.5, $\bar{M}_{nd}$ = 50 000, Φ_s = 0.6, and I_0 = 0.05 mol/L).

reactor model. It is shown that a solution to the optimal control problem can be obtained by iterating upon the initial value of one costate variable, thus avoiding the solution of the originally derived TPBVP. It should be noted that once the optimal control temperature has been found, the complete reactor model is used to calculate the time variation of conversion and number-average molecular weight. It is interesting to note that the optimal temperature policies obtained from the approximate model were almost identical with those calculated by the gradient method (Ponnuswamy, 1984).

The calculated optimal temperature policies were subsequently implemented on the experimental reactor system described previously. For this purpose, the calculated optimal policies were initially stored in a disk file and at the time of implementation were sent as remote set-point changes through a current output station to the local PI temperature controller. Conversion values were measured on-line by a densitometer and off-line by a gas chromatograph. $\bar{M}_n$ and $\bar{M}_w$ values were measured by a computer-operated size exclusion chromatograph (SEC). The experimental results (discrete points) along with the theoretical predictions (solid lines) are presented in Figure 2 for a minimum-time optimal temperature policy with X_d = 0.5 and $\bar{M}_{nd}$ = 50 000.

It can be seen that the reactor temperature closely follows the optimal temperature trajectory. As shown in Appendix I, the optimal policy, eq I.13, is one of increasing temperature so that the term $k_1 I^{1/2}$ remains constant. Thus, for conventional polymerization (i.e., low initiator conversion), the optimal temperature policy is almost isothermal. Similar results were reported by Sacks et al. (1972) and Chen and Jeng (1978). As a result, these time optimal temperature policies do not significantly reduce the polymerization time compared to the best isothermal policies derived from the solution of a simpler static optimization problem (Ponnuswamy, 1984).

Curves a, b, and c in Figure 2 show the corresponding conversion, $\bar{M}_n$, and polydispersity optimal profiles. Although the experimental values for $\bar{M}_n$ are lower than the theoretical values, this difference is not unreasonable
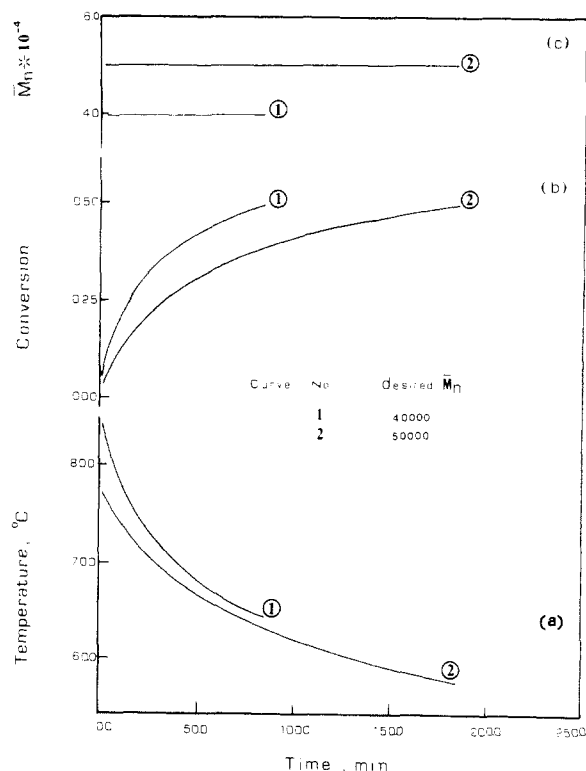

Figure 3. Minimum polydispersity optimal temperature (a), conversion (b), and number-average molecular weight (c) policies (X_d = 0.5, Φ_s = 0.6, and I_0 = 0.075 mol/L).

considering all possible sources of modeling and experimental errors. It should be noted that in similar model verification studies (Cutter and Drexler, 1982; Hamer, 1983), the reported experimental values for X, $\bar{M}_n$, and $\bar{M}_w$ differed from the corresponding theoretical values by as much as 50%.

The Minimum Polydispersity Temperature Policy

The objective in this problem is to calculate the temperature policy for a given initial initiator concentration to produce a polymer with minimum polydispersity and desired final values for X_d and $\bar{M}_{nd}$.

Hoffman et al. (1964) calculated some initiator and monomer addition policies required to produce a polymer product with minimum breadth of MWD. They reasoned that for a minimum polydispersity, the instantaneous number-average molecular weight had to be constant throughout the polymerization. Sacks et al. (1973) later proved mathematically Hoffman's reasoning. They also showed that in conventional polymerization (i.e., initiator concentration is almost constant), the optimal temperature policy turns out to be a decreasing temperature profile.

To calculate the minimum polydispersity temperature policy, the Maximum Principle was applied to the approximate mathematical model of the process. The mathematical derivation of the optimal policy along with the numerical procedure is given in Appendix II. As in the previous section, through the use of the approximate model, the computational procedure to obtain the optimal policy is greatly simplified.

In Figure 3, calculated optimal minimum polydispersity policies for two specified values of $\bar{M}_{nd}$ and the same value of X_d are plotted. An experimental verification of the second policy is shown in Figure 4. Discrete points indicate the experimental values of the variables, and the solid lines represent the calculated results. Apparently, there is close agreement between the theoretical and ex-
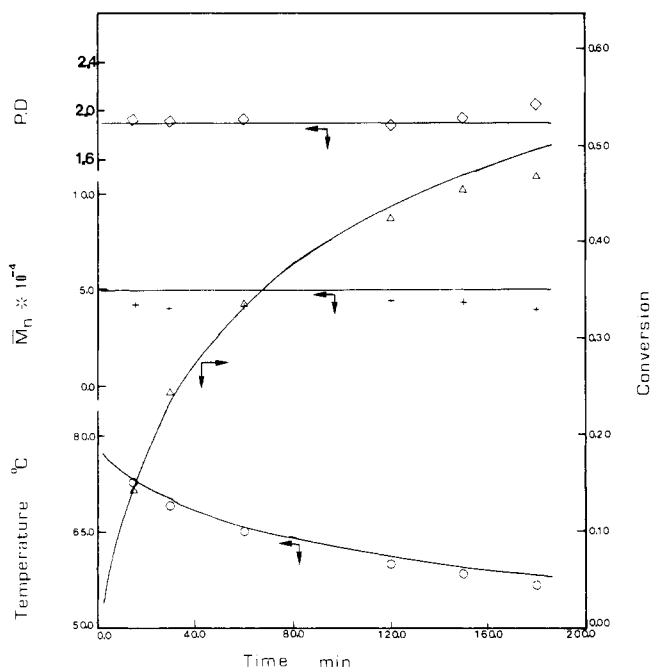
Figure 4. Comparison of theoretical and experimental results for a minimum polydispersity time optimal temperature policy (X_d = 0.5, $\bar{M}_{nd}$ = 50 000, Φ_s = 0.6, and I_0 = 0.075 mol/L).

perimental values which proves the validity of our calculations.

It can be seen that the temperature decreases with time during the course of polymerization, which agrees with earlier reported results by Sacks et al. (1973). Note that under a minimum polydispersity temperature policy, the instantaneous value of $\bar{M}_n$ remains constant (Figures 3 and 4).

Furthermore, it was found that as the final desired value of $\bar{M}_{nd}$ increases for a given value of X_d, the optimal temperature policy decreases, which brings about an increase in the total reaction time (Figure 3).

Closed-Loop Control Studies

Compared to open-loop optimal control studies, there have been reported only few applications on optimal closed-loop control of polymerization reactors (Kenat et al., 1967; Keyes and Kennedy, 1974; Jo and Bankoff, 1976; Kiparissides et al., 1981; Kiparissides and Ponnuswamy, 1981; Timm et al., 1982; Harris and Rushing, 1982; Arnold et al., 1980; Ponnuswamy et al., 1985; Tzouanas and Shah, 1985). This is mainly due to the lack of robust on-line measurements of process variables such as conversion, molecular weight distribution (MWD), and copolymer composition distribution (CCD).

In regulatory control, we are interested in keeping the process variables along the established optimal state trajectories in the presence of process disturbances. Assuming that accurate on-line measurements of the state variables are available, the closed-loop problem can be solved to calculate the optimal feedback control law that minimizes the deviations of state variables from their optimal values. This problem is discussed next.

Linear-Quadratic Feedback Control

The free-radical solution polymerization of MMA in a batch reactor can be described in terms of a set of nonlinear differential equations, (1)–(4). The ability of this model to provide reactor simulations by specifying reactor operating conditions has been demonstrated in the previous sections.

Our objective in this problem is to design a linear feedback controller so that the state variables M, μ_0, and μ_2 track the optimal trajectories M_s, μ_{0s}, and μ_{2s} despite the presence of disturbances in the initiator concentration. The optimal state and control trajectories are obtained by solving an open-loop optimal control problem as demonstrated previously.

The design of linear feedback controllers for linear, discrete state-space models is a well-known procedure. Analytical solutions to this problem are available for systems that can be formulated with a quadratic performance criterion:

$$J = \frac{1}{2} Y^T(N) W Y(N) + \frac{1}{2} \sum_{k=1}^{N-1} [Y^T(k)Q Y(k) + U^T(k)R U(k)] \quad (34)$$

where **W** and **Q** are positive, semidefinite weighting matrices and **R** is a positive definite matrix.

Assume that the state and control variables deviate slightly from their corresponding nominal trajectories. Then, we can expand the nonlinear functions on the right-hand sides of eq 1–4 by using the Taylor series in terms of the deviation variables. Neglecting the second-order and higher order terms and writing the equations in the standard vector–matrix form, we obtain the following result:

$$\dot{Y} = A(t) Y + B(t)U + D(t)V \quad (35)$$

where Y is a (3 × 1) state vector

$$Y = [(M - M_s), (\mu_0 - \mu_{0s}), (\mu_2 - \mu_{2s})]^T \quad (36)$$

U is the control variable and represents the deviation of the temperature from its nominal value, $(T - T_s)$. V is a disturbance variable, $(I - I_s)$, which can change with time but cannot be controlled. Finally, **A**, **B**, and **D** are (3 × 3), (3 × 1), and (3 × 1) matrices, respectively, found by linearization of the nonlinear model around the optimal trajectories. It should be noted that the elements of **A**, **B**, and **D** will depend on the nominal values of the state control trajectories, and hence they will vary with time.

Since the reactor is to be controlled directly by a digital computer, it will be more convenient to have a corresponding discrete state-space model. This can be easily obtained from the continuous linearized model 35 (Aström and Wittenmark, 1984; Franklin and Powell, 1981):

$$Y(k + 1) = F_k Y(k) + G_k U(k) + H_k V(k) \quad (37)$$

The discrete model matrices are calculated by

$$F_k = \exp(A_k \tau) \quad (38)$$

$$G_k = \int_0^\tau (\exp(A_k t) \, dt) B_k \quad (39)$$

$$H_k = \int_0^\tau (\exp(A_k t) \, dt) D_k \quad (40)$$

where τ is the sampling time interval. The reactor model was discretized based on a sampling time of 5 min. It was found that the linearized and discretized model responses closely followed the time responses of the nonlinear model (Ponnuswamy, 1984).

The optimal feedback control law for the linear discrete system 37 with quadratic performance index 34 is (Sage, 1968)

$$U_k = -K_k Y(k) \quad (41)$$

$$K_k = R^{-1} G_k^T [P_{k+1}^{-1} + G_k R^{-1} G_k^T]^{-1} F_k \quad (42)$$

$$P_k = Q + F_k^T [P_{k+1}^{-1} + G_k R^{-1} G_k^T]^{-1} F_k \quad (43)$$

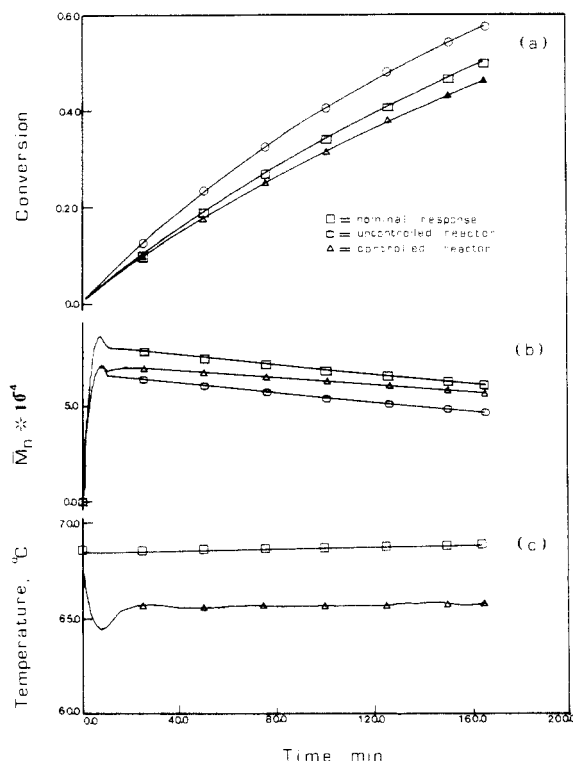$$P_N = W \qquad k = N, N-1, ..., 1 \quad (44)$$

Figure 5. Comparison of monomer conversion (a), number-average molecular weight (b), and temperature (c) nominal, uncontrolled, and controlled responses in the presence of a positive disturbance in the initial initiator concentration (I_0 = 0.05 mol/L, ΔI_0 = 0.025 mol/L, X_d = 0.5, $\bar{M}_{nd}$ = 60 000, Φ_s = 0.6).

The matrix difference eq 42 and 43 can be solved backward in time with the final condition 44. The off-line calculated elements of the gain matrix, $\mathbf{K}_k$, are called "Kalman gains" and are applied to the physical system as it runs forward in real-time. In what follows, simulation results are presented that demonstrate the ability of the derived controller to cope with the effects of step disturbances in the initiator concentration. For all simulated runs, the nominal control and state trajectories are calculated by solving the minimum time optimal temperature problem.

In Figure 5a, the nominal, uncontrolled, and controlled monomer conversion responses are plotted against the reaction time for the case of a positive step increase in the initial initiator concentration. The corresponding number-average molecular weight responses are plotted in Figure 5b. Figure 5c shows how the control variable, in this case the polymerization temperature, must vary from its nominal trajectory to maintain the state variables close to their nominal values. When the reactor operates under feedback control, the polymerization temperature decreases from its nominal optimal trajectory to counteract the effect of the positive increase in the initiator concentration. It can be clearly seen in parts a and b of Figure 5 that under feedback control the monomer conversion and number-average molecular weight responses move closer to their nominal optimal values.

Note that the derived feedback controller, eq 41, is of proportional type which could explain the observed offsets between the nominal and controlled responses. However, even the use of a multivariable PI controller will not likely remove the observed deviations in monomer conversion and $\bar{M}_n$ values since these variables react in opposite directions to manipulations of the temperature control variable (parts a and b of Figure 5).

Conclusions

This paper provides a detailed analysis of open-loop and closed-loop control of batch polymerization reactors.

The Maximum Principle is applied to a mathematical model of the polymerization process to derive optimal temperature and initiator addition policies required to produce a polymer with specified values of final monomer conversion and number-average molecular weight. Two of these optimal policies have been implemented on a fully automated experimental reactor system. A comparison of model and experimental results shows close agreement between theoretical and experimental conversion values, whereas a difference of about 20% is observed in the number-average molecular weight results. This discrepancy is well within the range of modeling and experimental errors reported by other investigators.

Linear multivariable control theory is also applied to a linearized reactor model to derive a feedback regulator to maintain the state variables along the optimal state trajectories in the presence of process disturbances. The successful application of the derived feedback controller to the simulated reactor model should provide a good criterion of its value on the real process.

Nomenclature

A_i = Arrhenius factor for the rate constant k_i
$\mathbf{A}$ = (3 × 3) state matrix in linear model
$\mathbf{B}$ = (3 × 1) control matrix in linear model
$\mathbf{D}$ = (3 × 1) disturbance matrix in linear model
E_i = activation energy for the rate constant k_i
f = initiator efficiency
$\mathbf{F}_k$ = (3 × 3) discrete state matrix
$\mathbf{G}_k$ = (3 × 1) discrete control matrix
$\mathscr{H}$ = Hamiltonian
$\mathbf{H}_k$ = (3 × 1) disturbance matrix in discrete model
I = initiator concentration, mol/L
I_0 = initial initiator concentration, mol/L
k_d = dissociation rate constant, $3.75 \times 10^{16} \exp(-33740/RT)$, s^{-1}
k_m = transfer to monomer rate constant, $3.88 \times 10^{14} \times \exp(-27603/RT)$, L/(mol·s)
k_p = propagation rate constant, $1.20 \times 10^9 \exp(-9630/RT)$, L/(mol·s)
k_s = transfer to solvent rate constant, $4.41 \times 10^{20} \times \exp(-34443/RT)$, L/(mol·s)
k_t = ($= k_{tc} + k_{td}$), termination rate constant, $2.113 \times 10^8 \times \exp(-1014/RT)$, L/(mol·s)
k_{tc} = termination by combination rate constant, L/(mol·s)
k_{td} = termination by disproportionation rate constant, L/(mol·s)
$\mathbf{K}_k$ = gain matrix
M = monomer concentration, mol/L
M_0 = initial monomer concentration, mol/L
$\bar{M}_n$ = number-average molecular weight
$\bar{M}_{nd}$ = desired number-average molecular weight
$\bar{M}_w$ = weight-average molecular weight
MW = molecular weight of the monomer
p_i = ith costate variable
$\mathbf{p}$ = costate vector
$\mathbf{Q}$ = (3 × 3) weighting matrix for state variables
$\mathbf{R}$ = weighting matrix for control variables
S = solvent concentration, mol/L
t = time, s
t_f = final time, s
T = temperature, K
V = volume of reaction mixture, eq 27
V = disturbance variable, eq 35
w = weight
$\mathbf{W}$ = (3 × 3) weighting matrix
X = conversion
X_d = desired conversion
U = control variable
Y = state vector

Greek Symbols

λ_i = ith moment of the live radical distribution
μ_i = ith moment of deal polymer distribution
ν = k_{tc}/k_t, constant
Φ_s = volume fraction of solvent

Appendix I: The Minimum-Time Approximate Temperature Policy

In this development, an approximate mathematical model obtained from eq 1–4 by neglecting the transfer to monomer and solvent reactions is used.

$$dI/dt = -k_d I \qquad (I.1)$$

$$dM/dt = -k_1 M I^{1/2} \qquad (I.2)$$

$$d\mu_0/dt = k_4 k_d I \qquad (I.3)$$

$$d\mu_2/dt = k_6 M^2 \qquad (I.4)$$

The objective of this problem is to find the time optimal temperature policy for a given initial initiator concentration and desired final values for X and $\bar{M}_n$ that minimizes the following performance index:

$$\min t_f = \max \left(-\int_0^{t_f} dt \right) \qquad (I.5)$$

Define the Hamiltonian of the system as

$$\mathcal{H} = -1 - p_1 k_d I - p_2 k_1 M I^{1/2} + p_3 k_4 k_d I \qquad (I.6)$$

where the costate variables p_1, p_2, and p_3 satisfy the following canonical equations:

$$dp_1/dt = -\partial\mathcal{H}/\partial I = p_1 k_d + \tfrac{1}{2} p_2 k_1 M I^{-1/2} - p_3 k_4 k_d \quad (I.7)$$

$$dp_2/dt = -\partial\mathcal{H}/\partial M = p_2 k_1 I^{1/2} \qquad (I.8)$$

$$dp_3/dt = -\partial\mathcal{H}/\mu_0 = 0 \qquad (I.9)$$

Assuming no constraint on the temperature, the necessary conditions for optimality are written as

$$\mathcal{H} = 0 \qquad (I.10)$$

$$\partial\mathcal{H}/\partial T =$$
$$(p_1 E_d k_d I + p_2 E_1 k_1 M I^{1/2} - p_3 k_4 E_d k_d I)/RT^2 = 0 \quad (I.11)$$

From eq I.2 and I.8, we obtain

$$dM/M + dp_2/p_2 = 0 \qquad p_2 M = \text{constant} = C \quad (I.12)$$

Combining eq I.10–I.12, we finally get

$$k_1 I^{1/2} = E_d/[C(E_1 - E_d)] \qquad (I.13)$$

The time optimal temperature is calculated by the following simple iterative procedure.

1. Assume an initial value for p_2 at time $t = 0$.
2. Calculate the value of C at time $t = 0$, eq I.12.
3. Integrate eq I.1–I.3 and at each increment solve eq I.13 to determine the optimal temperature.
4. At $X = X_d$, compare $\bar{M}_n$ to the desired value $\bar{M}_{nd}$. If these are within a maximum allowable error ϵ, terminate the iterative solution.
5. Otherwise adjust the value of $p_2(0)$, and return to step 2.

Appendix II: The Minimum Polydispersity Approximate Temperature Policy

The objective in this problem is to calculate the optimal temperature policy for a given initial initiator concentration and desired final values of X_d and $\bar{M}_{nd}$ that minimize the performance index

$$J = \mu_2(t_f) \qquad (II.1)$$

The Hamiltonian for this problem is defined as

$$\mathcal{H} = -p_1 k_d I - p_2 k_1 M I^{1/2} + p_3 k_6 M^2 \qquad (II.2)$$

where p_1, p_2, and p_3 are costate variables which must satisfy the canonical equations

$$dp_1/dt = -\partial\mathcal{H}/\partial I = p_1 k_d + p_2 k_1 M/(2I^{1/2}) \quad (II.3)$$

$$dp_2/dt = -\partial\mathcal{H}/\partial M = p_2 k_1 I^{1/2} - 2p_3 k_6 M \quad (II.4)$$

$$dp_3/dp_t = -\partial\mathcal{H}/\partial\mu_2 = 0 \qquad (II.5)$$

The initial and final conditions of the problem can be written as

variable	$t = 0$	$t = t_f$
I	I_0	$I_0 - M_0 X_d(MW)/k_4 M_{nd}$
M	M_0	$M_0(1 - X_d)$
μ_2	0	free
p_1	free	free
p_2	free	free
p_3	−1	−1

Along the optimal path, the following necessary conditions will hold good:

$$\partial\mathcal{H}/\partial T = (1/RT^2)(-p_1 E_d k_d I -$$
$$p_2 E_1 k_1 M I^{1/2} + p_3 E_6 k_6 M^2) = 0 \quad (II.6)$$

$$\mathcal{H} = -p_1 k_d I - p_2 k_1 M I^{1/2} + p_3 k_6 M^2 = 0 \quad (II.7)$$

From eq II.6 and II.7 and with $p_3 = -1$, we get

$$p_2 k_1 M I^{1/2}(E_d - E_1) - k_6 M^2(E_6 - E_d) = 0 \quad (II.8)$$

where

$$k_6 = (2 + \nu)k_p^2/k_t = A_6 \exp(-E_6/RT) \quad (II.9)$$

$$k_1 = k_p(2f k_d/k_t)^{1/2} = A_1 \exp(-E_1/RT) \quad (II.10)$$

Assuming a value of $f = 0.5$, from eq II.9 and II.10, we obtain

$$E_6 - E_d = -2(E_d - E_1) \qquad (II.11)$$

Substituting eq II.11 into eq II.8 and rearranging, we get

$$k_1/k_6 = -2MI^{-1/2}/p_2 \qquad (II.12)$$

Finally, from eq II.9, II.10, and II.12, the optimal temperature (T) can be calculated as

$$T = \frac{E_6 - E_1}{R \ln [-2A_6 M/(A_1 p_2 I^{1/2})]} \qquad (II.13)$$

The optimal temperature profile is computed by the following procedure.

1. Assume $p_2(0)$.
2. Calculate T from eq II.13.
3. Integrate eq I.1–I.3 until the desired conversion (X_d) is reached.
4. Check if $\bar{M}_n$ has reached the desired value, $\bar{M}_{nd}$. If these values are within a maximum allowable error, ϵ, terminate the iterative solution.
5. Otherwise adjust the value of $p_2(0)$, and return to step 2.

Registry No. PMMA, 9011-14-7.

Literature Cited

Amrehn, H. *Automatica* **1977**, *13*, 533.
Arnold, K.; Johnson, A. F.; Ramsay, J. *Proceedings of the 4th IFAC-PRP Automation Conference*; Van Cauwenberghe, A., Ed.; Pergamon: Belgium, 1980; p 359.
Åström, K. J.; Wittenmark, B. *Computer Controlled Systems*; Prentice Hall: Englewood Cliffs, NJ, 1984.
Chen, S.; Hsu, K. *Chem. Eng. Sci.* **1984**, *39*, 177.
Chen, S.; Huang, N. *Chem. Eng. Sci.* **1981**, *36*, 1295.
Chen, S.; Jeng, W. *Chem. Eng. Sci.* **1978**, *33*, 735.

Chen, S.; Lin, K. *Chem. Eng. Sci.* **1980,** *35,* 2325.

Cutter, L. A.; Drexler, T. D. *Am. Chem. Soc. Symp. Ser.* **1982,** *197,* 13.

Farber, J. N. Ph.D. Thesis, University of Massachusetts, Amherst, 1983.

Franklin, G. F.; Powell, J. D. *Digital Control of Dynamic Systems*; Addison-Wesley: Menlo Park, CA, 1981.

Hamer, J. W. Ph.D. Thesis, University of Wisconsin, Madison, 1983.

Harris, T. J.; Rushing, E. V. Paper presented at the AIChE National Meeting in Orlando, FL, 1982.

Hicks, J.; Mohan, A.; Ray, W. H. *Can. J. Chem. Eng.* **1969,** *47,* 590.

Hoffman, R. F.; Schreiber, S.; Rosen, G. *Ind. Eng. Chem. Fundam.* **1964,** *56,* 51.

Hoogendoorn, K.; Shaw, R. *Proceedings of the 4th IFAC-PRP Automation Conference*; Van Cauwenberghe, A., Ed.; Pergamon: Belgium, 1980; p 623.

Jo, J. H.; Bankoff, S. G. *AIChE J.* **1976,** *22,* 361.

Kenat, T. A.; Kermode, R. I.; Rosen, S. L. *Ind. Eng. Chem. Proc. Des. Dev.* **1967,** *6,* 363.

Keyes, M. A.; Kennedy, J. P. Proceedings of the 2nd Purdue Conference on Process Control, New York, 1974, p 89.

Kiparissides, C.; MacGregor, J. F.; Hamielec, A. E. *AIChE J.* **1981,** *27,* 13.

Kiparissides, C.; Ponnuswamy, S. R. *Can. J. Chem. Eng.* **1981,** *59,* 752.

Kirk, D. E. *Optimal Control Theory*; Prentice Hall: Englewood Cliffs, NJ, 1970.

MacGregor, F. J.; Hamielec, A. E.; Penlidis, A. Proceedings of the 5th IFAC-PRP Conference, Antwerp, Belgium, 1983, p 291.

Ponnuswamy, S. R. Ph.D. Thesis, University of Alberta, Edmonton, Canada, 1984.

Ponnuswamy, S. R.; Shah, S. L.; Kiparissides, C. Proceedings of the 1985 ACC, Boston, 1985.

Ponnuswamy, S. R.; Shah, S. L.; Kiparissides, C. *J. Appl. Polym. Sci.* **1986a,** *32,* 3239.

Ponnuswamy, S. R.; Shah, S. L.; Kiparissides, C. *J. Liq. Chromatogr.* **1986b,** *9,* 2411.

Ray, W. H. *Can. J. Chem. Eng.* **1967,** *45,* 356.

Sacks, M. E.; Lee, S.; Biesenberger, J. A. *Chem. Eng. Sci.* **1972,** *27,* 2281.

Sacks, M. E.; Lee, S.; Biesenberger, J. A. *Chem. Eng. Sci.* **1973,** *28,* 241.

Sage, A. P. *Optimum Systems Control*; Prentice Hall: Englewood Cliffs, NJ, 1968.

Schork, F. J.; Ray, W. H. *Am. Chem. Soc. Symp. Ser.* **1981,** *165,* 505.

Thomas, I.; Kiparissides, C. *Can. J. Chem. Eng.* **1984,** *62,* 284.

Timm, D. C.; Gilbert, R. E.; Ko, T. T.; Simmons, M. R. *Am. Chem. Soc. Symp. Ser.* **1982,** *197,* 3.

Tirrell, M.; Gromley, K. *Chem. Eng. Sci.* **1981,** *36,* 367.

Tsoukas, A.; Tirrell, M.; Stephanopoulos, G. *Chem. Eng. Sci.* **1982,** *37,* 1785.

Tzouanas, V.; Shah, S. L. Proceedings of the 1985 IFAC Conference on Adaptive Control of Chemical Processes, Frankfurt, Germany, 1985, p 114.

Wu, G. Z. A.; Denton, L. A.; Laurence, R. L. Paper presented at the Annual AIChE Meeting in Chicago, 1980.

Yoshimoto, Y.; Yanagawa, H.; Suzuki, T.; Araki, T.; Inaba, Y. *Int. Chem. Eng.* **1971,** *11,* 147.

Kinetic Investigation and Reactor Simulation for the Catalytic Gas-Phase Oxidation of *n*-Butane to Maleic Anhydride

P. Schneider

Enka AG, D-8573 Obernburg, West Germany

G. Emig* and H. Hofmann*

Institute of Technical Chemistry I, University of Erlangen—Nürnberg, D-8520 Erlangen, West Germany

Kinetic investigations on *n*-butane oxidation on a V–P–O catalyst prepared in an aqueous solution are presented. The complex reaction could be described accurately enough by three parallel reactions leading to maleic anhydride, CO, and CO_2. The rates of the different reactions have been modeled by an Eley–Rideal mechanism more suitable than by a Mars–Van Krevelen mechanism. Simulation and optimization of technical tube bundle and fluidized bed reactors have been performed on the basis of these kinetic results.

While numerous publications deal with the mechanism of the *n*-butane oxidation reaction to maleic anhydride according to
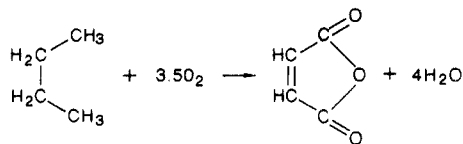
and the role of oxidic catalysts (Moser and Schrader, 1985; Hodnett, 1985; Volta and Portefaix 1985), one hardly finds published works about the quantitative investigations of the kinetics and reaction engineering considerations for the optimal design of this reaction (Centi et al., 1985; Escardino et al., 1973). The large number of recipes for the production of industrially relevant vanadium–phosphorus oxide catalysts for this reaction can be divided up into two groups: catalysts prepared in an aqueous solution or alternatively in an alcoholic solution. In this work, we intended to report about the kinetics with a catalyst prepared in an aqueous medium. We shall further demonstrate by simulation of possible reactor configurations how this catalyst can be attractive for industrial application.

Experimental Equipment

The experimental investigations (Schneider, 1985) were conducted in a gradientless recycle reactor with an external recycle loop (Figure 1). Approximately 3 g of catalyst having a particle size between 0.8 and 1.2 mm was introduced into the reactor; a metal bellow pump (Metal Bellows, type MB-158 HT) recycled the gas and was mounted in a hot air thermostat (operating temperature, 170 °C) together with the gas sampling valve, in order to avoid condensation. All other external tubing was also heated